



HAL
open science

Solid-state formation of CO and H₂CO via the CHOCHO + H reaction

Killian Leroux, Jean-Claude Guillemin, Lahouari Krim

► **To cite this version:**

Killian Leroux, Jean-Claude Guillemin, Lahouari Krim. Solid-state formation of CO and H₂CO via the CHOCHO + H reaction. *Monthly Notices of the Royal Astronomical Society*, 2020, 491 (1), pp.289-301. 10.1093/mnras/stz3051 . hal-02485745

HAL Id: hal-02485745

<https://hal.sorbonne-universite.fr/hal-02485745>

Submitted on 20 Feb 2020

HAL is a multi-disciplinary open access archive for the deposit and dissemination of scientific research documents, whether they are published or not. The documents may come from teaching and research institutions in France or abroad, or from public or private research centers.

L'archive ouverte pluridisciplinaire **HAL**, est destinée au dépôt et à la diffusion de documents scientifiques de niveau recherche, publiés ou non, émanant des établissements d'enseignement et de recherche français ou étrangers, des laboratoires publics ou privés.

Solid-state formation of CO and H₂CO via the CHOCHO + H reaction

Killian Leroux¹, Jean-Claude Guillemin² and Lahouari Krim^{1*}

¹*Sorbonne Université, CNRS, De la Molécule aux Nano-Objets: Réactivité, Interactions, Spectroscopies, MONARIS, 75005, Paris, France.*

²*Univ Rennes, Ecole Nationale Supérieure de Chimie de Rennes, CNRS, ISCR – UMR6226, F-35000 Rennes, France.*

* *Corresponding author: Lahouari.krim@upmc.fr*

Abstract:

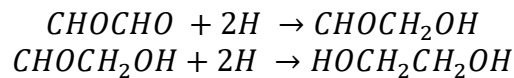
Glycolaldehyde (CHOCH₂OH) and ethylene glycol (HOCH₂CH₂OH) are among many complex organic molecules (COM) detected in the interstellar medium (ISM). Astrophysical models proposed very often that the formation of these compounds would be directly linked to the hydrogenation of glyoxal (CHOCHO), a potential precursor which is not yet detected in the ISM. We have performed, in the present work, surface and bulk hydrogenations of solid CHOCHO under ISM conditions in order to confirm or invalidate the astrophysical modeling of glyoxal transformation. Our results show that the hydrogenation of glyoxal does not lead to the formation of detectable amounts of heavier organic molecules such as glycolaldehyde and ethylene glycol but rather to lighter CO-bearing species such as CO, H₂CO and CO-H₂CO, a reaction intermediate resulting from an H-addition-elimination process on CHOCHO and where CO is linked to H₂CO. The solid phase formation of such a reaction intermediate has been confirmed through the neon matrix isolation of CO-H₂CO species. Additionally, the CHOCHO + H solid state reaction might also lead to the production of CH₃OH formed under our experimental conditions as a secondary product resulting from the hydrogenation of formaldehyde.

Keywords:

astrochemistry – methods: laboratory – techniques: spectroscopic – ISM: molecules

1 INTRODUCTION

Around 200 molecules have been detected in the interstellar medium (ISM) and circumstellar shells. Among them, more than 70 species containing six or more atoms of C, H, O or N (Herbst & van Dishoeck 2009) are called Complex Organic Molecules (COMs). Many of the COMs detected in the ISM are chemically linked through energetic and non-energetic processing and may be involved in a complex prebiotic chemistry. HCO, one of the simplest organic radical, has been detected in the four galactic molecular clouds W3, NGC 2024, W51, and K3-50 (Snyder et al. 1976) and more recently in the ISM toward the Blazars BL Lac and 3C 111 (Liszt et al. 2014), in prestellar cores (Frau et al. 2012; Becmann & Faure, 2015) and in the solar-type protostellar binary IRAS 16293–2422 (Rivilla et al. 2018). Naturally astrophysical models suggest that such a radical would either recombine to an H atom to form H₂CO or dimerize to form glyoxal CHOCHO (Wood et al. 2013) through non-energetic reactions which do not involve external energy to induce the chemical transformation of species detected in the ISM and which dominate the chemistry of the dark molecular clouds. Consequently, we would expect to detect both H₂CO and CHOCHO in the HCO-rich regions of the ISM. In contrast with H₂CO which is considered as the first COM detected in the ISM (Snyder et al. 1969), glyoxal has never been observed, opening all sorts of inquiries regarding its formation and reactivity in the ISM. The recurrent hypothesis is that glyoxal would be unstable under ISM conditions and would react efficiently with atomic hydrogen to form more COMs (Wood et al. 2013; Butscher et al. 2015). Indeed, many astrophysical models (Fedoseev et al. 2015, Wood et al. 2013) propose the formation of glycolaldehyde and ethylene glycol through successive hydrogenation of glyoxal:



In this way, glycolaldehyde and ethylene glycol have been detected in different regions of the ISM, which was not the case for their supposed precursor, glyoxal. Glycolaldehyde has been detected for the first time toward the galactic centre cloud Sagittarius B2(N) (Hollis et al. 2000). Since then, it has been detected outside the galactic center towards the hot molecular core G31.41 + 0.31 (Beltrán et al. 2009), around solar-type protostars, the Class 0 protostellar binary IRAS 16293-2422 (Jørgensen et al. 2010) and NGC 1333 IRAS2A (Coutens et al. 2015; Taquet et al. 2015). Similarly, ethylene glycol has been detected toward Sagittarius B2 (N-LMH) (Hollis et al. 2002) and around the Class 0 protostellar binary IRAS 16293-2422 (Jørgensen et al. 2010) and also in comet Hale-Bopp (Crovisier et al. 2004) and recently in the

hot core of Orion-KL (Brouillet et al. 2015). Even though its non-detection remains baffling, glyoxal has been extensively studied. It is regarded as a COM with two carbonyl groups in cis and trans configuration and it has been the subject of several theoretical and experimental investigations. Ha studied the cis-trans isomerization (Ha 1972) in glyoxal around the C-C bond. Figure 1 shows the relative energy of glyoxal isomers versus rotational angle of one OCH group around the C-C axis.

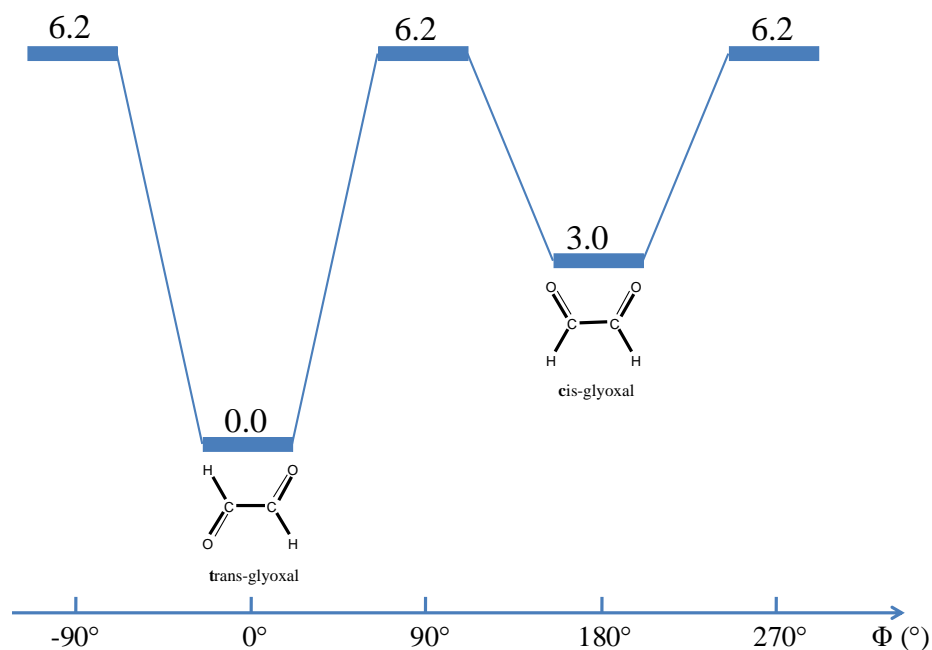


Figure 1: Relative energy (kcal/mol) of glyoxal conformers versus rotational angle (Φ) of one OCH group around the C-C axis (according to (Ha 1972)).

From figure 1, one can notice that the trans-glyoxal is more stable than the cis-glyoxal by 3 kcal/mol while the trans \rightarrow cis conversion would occur through an energy barrier of 6.2 kcal/mol. Consequently, in the coldest region of the dense molecular clouds, glyoxal would be present in the trans form with a null dipole moment which makes very difficult its astronomical detection but not that of its isotopomers. While in UV-rich regions of the ISM, both trans and cis forms would exist and due to its large dipole moment (4.3 Debye) the cis-glyoxal should be more easily detectable. Koch et al (Koch et al. 2001) calculated the activation energy of trans \rightarrow cis conversion at 0 and 300 K around 5.6 and 5.4 kcal/mol, respectively, showing that even at room temperature the glyoxal exists in its trans form with the [cis]/[trans] abundance ratio less than 1/1000. The aim of the present study is to investigate the hydrogenation of trans-glyoxal under ISM conditions, in order to monitor the behavior of a COM with two CO groups under H attacks.

2 EXPERIMENTAL SECTION

Glyoxal has been prepared as previously reported starting from trimeric glyoxal dihydrate and phosphorus (V) oxide (Wang et al. 1994). Hydrogen (99.9995 %) and Neon (99.9995 %) gases were purchased from Messer. The hydrogenation of glyoxal in solid state has been carried out through three different experiments:

- Exp 1, CHOCHO + H surface reaction: bombardment of a glyoxal ice by H-atoms at 10 K.
- Exp 2, CHOCHO + H bulk reaction: co-injection of glyoxal and H-atoms at 10 K.
- Exp 3, CHOCHO + H neon matrix isolated: co-injection of glyoxal diluted in neon gas and H-atoms at 3K.

The solid samples are formed in an ultrahigh vacuum chamber maintained at 10^{-10} mbar by condensation of gas reactants on a Rh-plated copper mirror maintained at 3 or 10 K (depending on the experiment) using a closed-cycle helium cryogenerator (Sumitomo cryogenics F-70) and programmable temperature controller (Lakeshore 336). At room temperature, the vapour pressures of aldehydes are approximately (Stull 1947) a few hundred mbars (glyoxal 293 mbar). That is why before introduction into the injection ramp, the glyoxal reservoir is cooled down to -50°C using a cooling bath made of liquid nitrogen and acetone. Afterwards, the frozen glyoxal is partially evaporated into the injection ramp by monitoring the bath temperature between -50 and 5°C . Pressures in the injection ramp are measured with a digital Pirani gauge while the fractions of glyoxal gas injected into the experimental chamber are controlled using a leak valve. H-atoms are formed by passing pure molecular hydrogen through a microwave driven atomic source (SPECS,PCS-ECR) while the pressures in the substrate chamber and source chamber during the atom-beam operation are 10^{-5} and 10 mbar, respectively. The H_2 dissociation yields are measured around 15 % using a Quadrupole Mass Spectrometer (QMS - Hidden Analytical) by monitoring the H and H_2 mass signals with the microwave discharge on and off. The H atoms flux of 10^{17} atoms cm^{-2} s^{-1} has been estimated from the amount of molecular hydrogen injected during the H-bombardment. The microwave discharge has been modified by adding to its output a curved Teflon tube. In fact, the curved Teflon allows to thermalize the species released from the atomic source and also to block the light from the plasma discharge to avoid possible photo-irradiation processing during the H-bombardment of our samples. In Exp 1, glyoxal ices are formed at 10 K and bombarded afterwards by H-atoms during 45 min while in Exp 2 and Exp 3, H-atoms are co-injected with pure glyoxal (during 30 min) and glyoxal/neon (during 20 min), respectively. In order to have the same amount of glyoxal in our samples in Exp 1 and Exp 2,

the glyoxal is deposited in a few seconds at 10^{-7} mbar for Exp 1, while for the co-injection experiment the glyoxal is injected at 9×10^{-9} mbar with a flux of $2 \mu\text{mol}/\text{min}$ leading to a ratio between H-atoms and glyoxal molecules equal to 150. In Exp 3, Neon cage is chosen as a matrix to isolate the CHOCHO + H reaction products and to characterize the reaction intermediates during the hydrogenation processes. Processing on the samples are probed in the mid infrared spectral region $4000\text{-}500 \text{ cm}^{-1}$ with a resolution of 0.5 cm^{-1} , using a Bruker Vertex 80v Fourier transform infrared (FTIR) spectrometer in the transmission–reflection mode with an incidence angle of 8° (Pirim & Krim 2011). We also use the temperature programmed desorption (TPD) method, monitored by spectrometry to characterize the CHOCHO + H reaction products formed in the solid phase and releasing in the gas phase during the thermal desorption of the solid sample.

3 RESULTS

Figures 2a and 2b show the IR spectra of glyoxal ice formed at 10 K, before and after H-bombardments, respectively. The assignments of the main vibrational modes are directly reported in figure 2 and table 1. The most characteristic IR signal of glyoxal molecule and corresponding to the C=O functional group is observed at 1709 cm^{-1} . Those corresponding to C-H stretching and CC-H bending modes are detected at 2865 and 1326 cm^{-1} , respectively.

Table 1 : Assignments of IR absorption bands of glyoxal ice

Vibration mode	Present work	Ref ^{a,b,c}
C-H stretch	2865	2852
C=O stretch	1709	1707
CC-H bend	1365	1361
CC-H bend	1326	1326
C-C stretch	1072	1078
C-H wagging	1053	1050
C-H wagging	818	842
Overtone band (C=O _{stretch})	3430	3422
Combination band (C=O _{stretch} + CC-H _{bend})	3063	3064
Combination band (C-C _{stretch} + C=O _{stretch})	2785	2786
Overtone band (CC-H _{bend})	2669	2677
Combination band (C=O _{stretch} + C-H _{wagg})	2393	2405
Overtone band (C-H _{wagg})	2085	2109
Combination band (C-C _{stretch} + C-H _{wagg})	1880	1891

^a(Cole & Durig 1975)

^b(Cole & Osborne 1971)

^c(Durig & Hannum 1971)

Figure 2b shows the results of the H-bombardments of glyoxal ice during 45 min. Figure 2c shows the difference spectrum before and after H-bombardments of CHOCHO ice, while in figure 2d, the IR spectrum of glycolaldehyde (CHOCH₂OH) ice, formed at 10 K under our experimental conditions, is shown as a reference spectrum for the reaction product we are supposed to obtain during the hydrogenation of CHOCHO ice. We notice by comparing figures 2c and 2d that there is no evidence for glycolaldehyde formation through H-bombardments of glyoxal ice. In fact, figure 2c shows no new signal indicating the presence of glycolaldehyde in our sample after hydrogenation processes. As shown in figure 2d, glycolaldehyde has two IR features at 3369 and 1745 cm⁻¹ (Hudson et al. 2005) due to OH and CO functional groups. The C=O functional group of glyoxal molecule shows a wide absorption band which may hide the signal of the reaction product at 1745 cm⁻¹, however no other signals characteristic of CHOCH₂OH are observed in the difference spectrum of figure 2c.

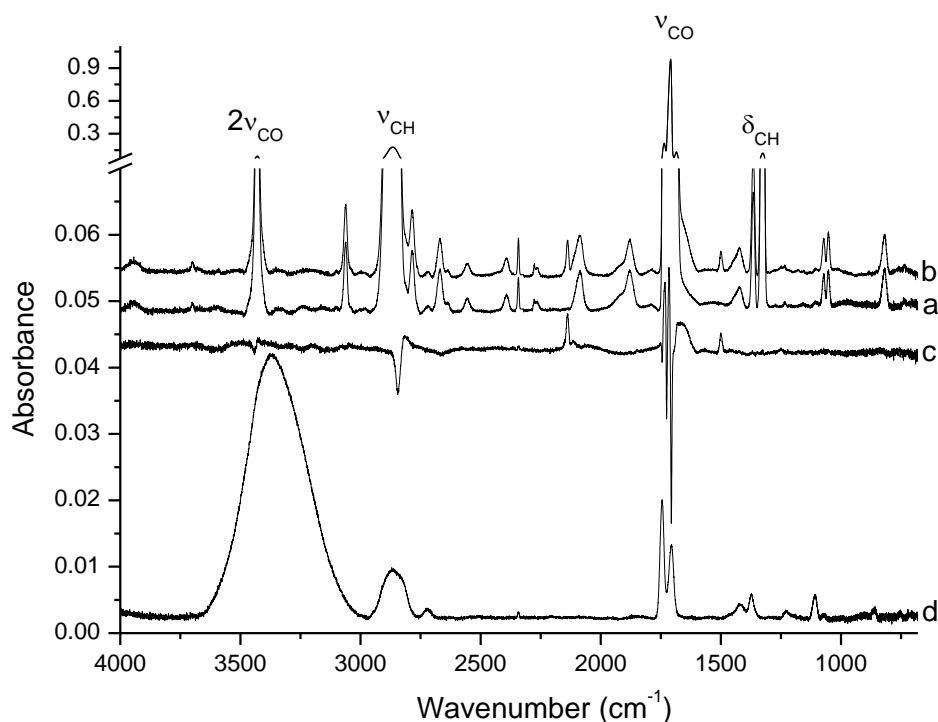


Figure 2: a) IR spectrum of glyoxal ice formed at 10 K (ν and δ refer to the stretching and bending modes, respectively). b) IR spectrum of glyoxal ice after H-bombardments. c) Difference spectrum before and after H-bombardments of CHOCHO. d) Deposition of pure glycolaldehyde (CHOCH₂OH) on a mirror maintained at 10 K.

Only two new absorption bands are clearly observed at 2138 and 1500 cm⁻¹ in the difference spectrum of figure 2c and also in the IR spectrum of glyoxal ice after H-bombardments

(figure 2b). These new IR signals cannot be assigned to the partially saturated glycolaldehyde or even to the totally saturated ethylene glycol ($\text{HOCH}_2\text{CH}_2\text{OH}$). Ethylene glycol has three characteristic IR signals at 3178, 1087 and 1049 cm^{-1} (Buckley & Giguère 1966, Hudson et al. 2005) which do not correlate with the new absorption bands we observe after H-bombardments of CHOCHO ice. Figure 3 exposes the zoom of figures 2a, 2b and 2c in two spectral regions, $2200\text{--}2000\text{ cm}^{-1}$ and $1550\text{--}1000\text{ cm}^{-1}$ where the two new IR bands appear as the only signals belonging to the reaction products from the H-bombardments of glyoxal ice. These two new signals may be easily assigned to CO (Ewin & Pimentel 1961, Gerakines et al. 1995) and H_2CO (Nelander 1980, Schutte et al. 1993) species, respectively. Another feature of H_2CO at 1250 cm^{-1} is observed as a tiny peak in Figure 2c. Similarly, the wide absorption band of C=O functional group of glyoxal may hide that of H_2CO , however the band at 1500 cm^{-1} is strong enough to be characteristic of formaldehyde formation.

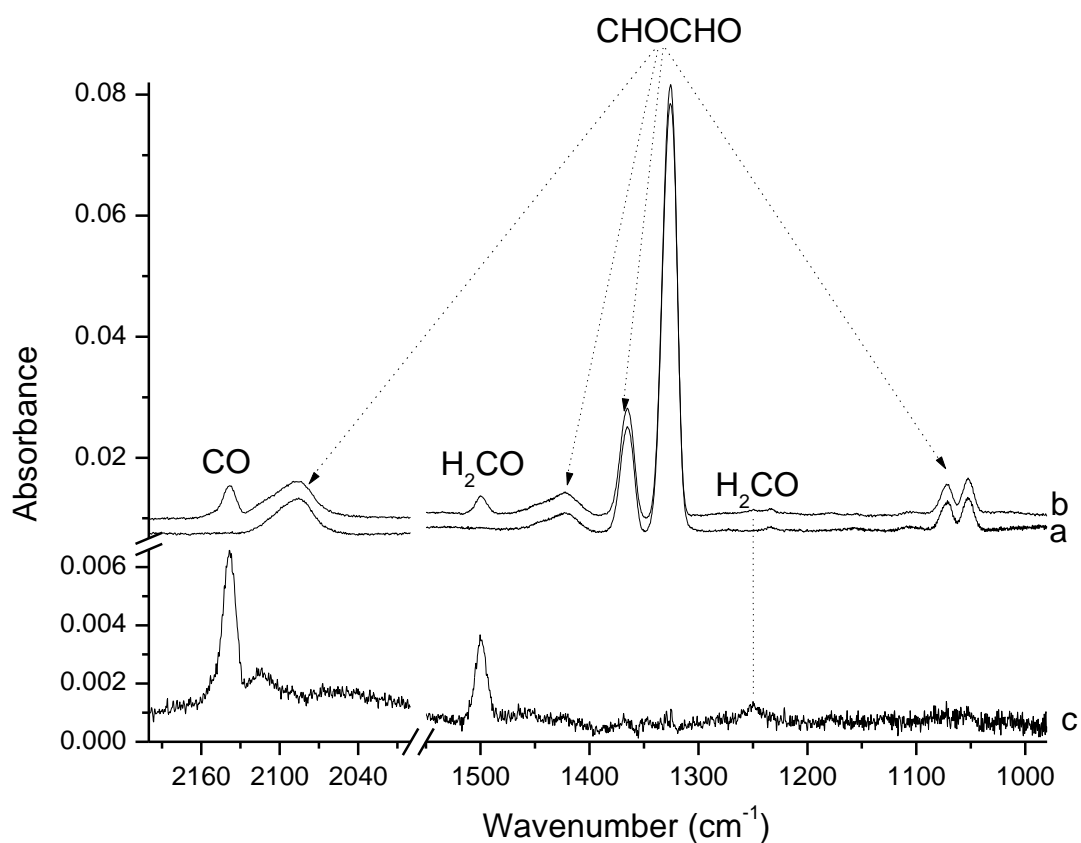


Figure 3: Zoom of figures 2a, 2b and 2c, in two spectral regions, $2200\text{--}2000\text{ cm}^{-1}$ and $1550\text{--}1000\text{ cm}^{-1}$. IR spectrum of glyoxal ice formed at 10 K, a) before H-bombardment. b) after 45 min H-bombardment. c) Difference spectrum before and after H-bombardments of CHOCHO

The first conclusion of the present study is that $\text{CHOCHO} + \text{H}$ solid state reaction leads to the formation of CO and H_2CO rather than glycolaldehyde or ethylene glycol. Glycolaldehyde is supposed to form through reduction of one of the CO functional group of CHOCHO . The fragmentation of glyoxal into CO and H_2CO and the non-formation of CHOCH_2OH during the H-bombardment of glyoxal ice would be due to the fact that all the processes occur on the first layer of sample surface. In the experimental configuration of Exp 1, there would be not enough bodies to absorb the energy excess released during the hydrogenation processing to prevent the reaction products from fragmentation. This is why we have carried out Exp 2 of $\text{CHOCHO}/\text{H}/\text{H}_2$ co-injection at 10K, where CHOCHO , H and H_2 are co-deposited simultaneously during 30 min. In the co-injection experiment, the H-atom flux has been kept similar to that of the H-bombardment experiments, while flux of CHOCHO has been monitored to reach in 30 min almost the same ice thicknesses as those of glyoxal ices which have been subjected to H-bombardment in Exp 1. In addition to stabilize the reaction products in the ice bulk made of H_2 and CHOCHO , the co-injection experiment would also increase the interaction probability between the reactants namely H-atoms and CHOCHO molecules.

Figure 4b shows the IR spectrum resulting from the $\text{CHOCHO}/\text{H}/\text{H}_2$ co-injection at 10 K. As a reference spectrum, figure 4a shows the IR spectrum corresponding to the CHOCHO/H_2 co-injection. Naturally, the reference spectrum of figure 4a is exactly similar to the IR spectrum of glyoxal ice shown in figure 2a, as there is no chemical reaction between CHOCHO and H_2 at 10 K. The comparison between the two IR spectra of figures 4a and 4b would allow to discriminate all the IR signals deriving from $\text{CHOCHO} + \text{H}$ reaction products. From this comparison, we notice that in addition to the CO and H_2CO IR signals we have already detected through the H-bombardment of glyoxal ice, additional IR signals appear during the $\text{CHOCHO}/\text{H}/\text{H}_2$ co-injection experiment.

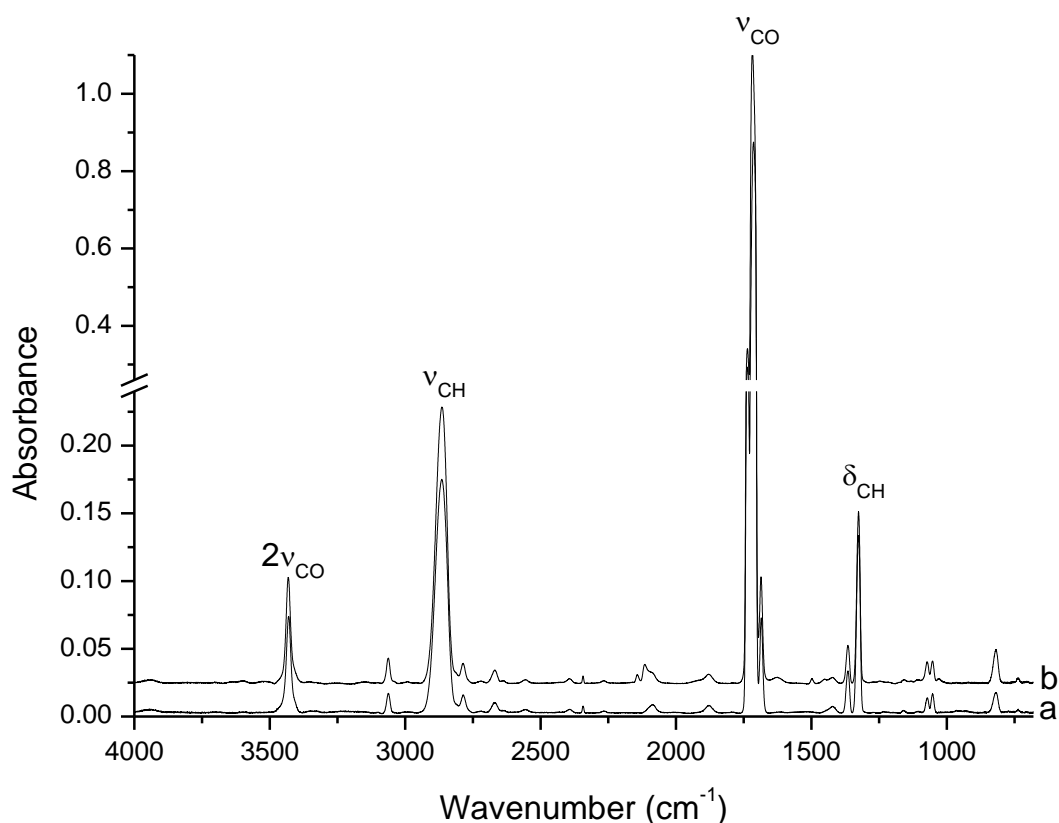


Figure 4 : Co-injection experiment during 30 min at 10 K. a) CHOCHO + H₂ reaction. b) CHOCHO + H+H₂ reaction.

Figure 5, a zoom of figure 4, shows the two IR spectral regions where the reaction products derived from CHOCHO + H solid state reaction are clearly identifiable. The new IR signals are located at 1029, 1452 and 2115 cm⁻¹. Many alcohol species show intense absorption bands (Buckley & Giguère 1966, Palumbo et al. 1999, Hudson et al. 2005, Maté et al. 2009, Butscher et al. 2015) in the 1000-1100 cm⁻¹ spectral region such as CH₃OH (at 1029 cm⁻¹), CHOCH₂OH (at 1071 and 1107 cm⁻¹) and HOCH₂CH₂OH (1087 and 1049 cm⁻¹). Consequently the new signal at 1029 cm⁻¹ might belong more to CH₃OH. However the absence of the characteristic OH absorption band in the 3000-3500 cm⁻¹ (figure 4b) allows only a tentative assignment of the band at 1029 cm⁻¹ to methanol which may be formed in very low amount as secondary reaction product due to the hydrogenation of H₂CO, the primary reaction product derived from CHOCHO + H reaction. The two other IR signals at 1452 and 2115 cm⁻¹, located in the CO and H₂CO molecules spectral regions, respectively, may be attributed to CO-H₂CO reaction intermediate, resulting from an H-addition-elimination reaction through CHOCHO + H → CO-H₂CO + H. More than a molecular

complex absorbing in the CO and H₂CO spectral region, the CO-H₂CO is a reaction intermediate where CO and H₂CO would be linked. In fact the intensities of these two absorption bands are temperature dependent. They start decreasing during the heating of the sample to 60 K and vanish completely when the sample temperature reaches 100 K. When the sample temperature increases above 60 K, the CO signal starts decreasing because of the CO desorption (Muñoz Caro et al. 2018) while the signal of H₂CO slightly increases. This shows that the sample heating from 10 to 100 K splits the CO-H₂CO bonding leading to free CO and H₂CO.

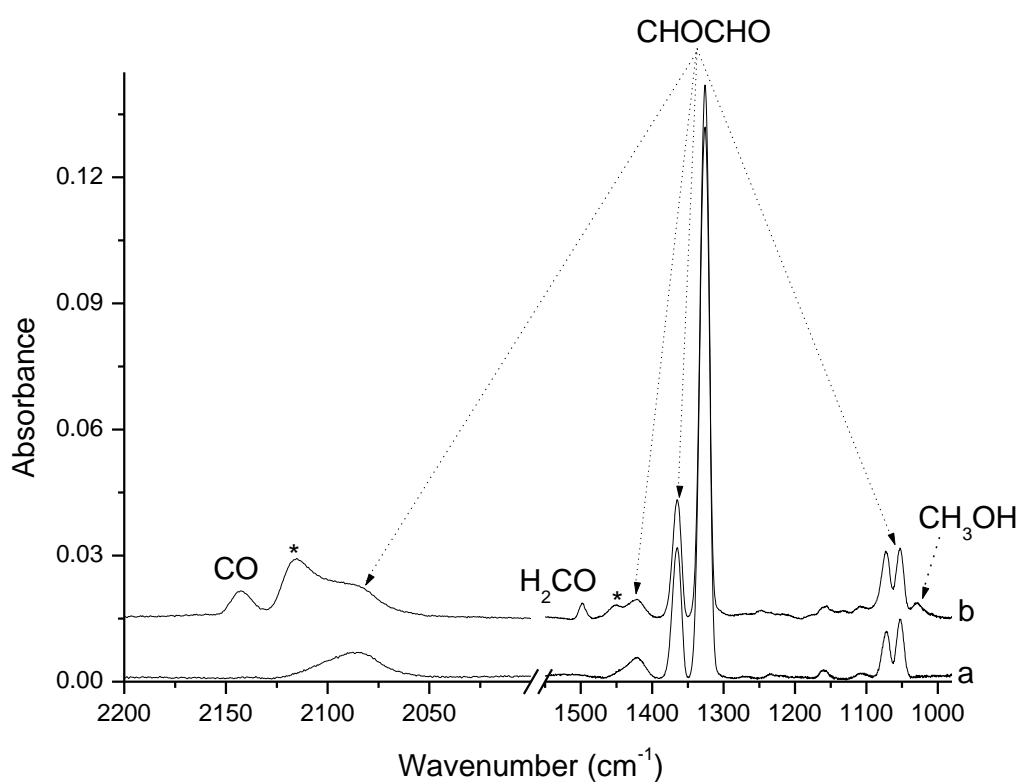


Figure 5: Zoom of figure 4, in two spectral regions, 2200-2000 cm⁻¹ and 1550-1000 cm⁻¹. a) CHOCHO + H₂ reaction. b) CHOCHO + H + H₂ reaction. Absorption bands labelled with a star belong to CO-H₂CO reaction intermediate (see in text).

Consequently, the CHOCHO + H/H₂ co-injection experiment leads to the identification of three reaction products namely, CO, H₂CO and CH₃OH, in addition to CO-H₂CO reaction intermediate which is stable only at temperatures lower than 60 K. As mentioned earlier, the new signal observed at 1029 cm⁻¹ observed only in Exp 2 is tentatively assigned to CH₃OH. This signal disappears when the sample is heated at 150 K which corresponds to desorption

temperature (145 K) of methanol (Maity et al. 2015). CH_3OH is suggested to be formed as a secondary reaction product through the hydrogenation of H_2CO which should be formed in enough amount in order to consider the competition between $\text{H}_2\text{CO} + \text{H}$ and $\text{CHOCHO} + \text{H}$ reactions. The comparison between Figures 3 and 5 shows that we form slightly the same amount of "free" H_2CO and CO in Exp 1 and Exp 2. However, we have to consider the fact that co-injection experiment lasts 30 min while in Exp 1 the CHOCHO ice is bombarded by H-atoms during 45 min. Additionally, the presence of new signals observed only in the co-injection experiments at 1452 and 2115 cm^{-1} and assigned to a species where CO is linked H_2CO indicates that in Exp 2 we would form more H_2CO which may be converted into CH_3OH .

In order to better characterize the $\text{CO-H}_2\text{CO}$ species and other probable reaction intermediates, we have investigated Exp 3, the neon matrix isolation of $\text{CHOCHO} + \text{H}$ reaction which would allow to observe both reaction products and reaction intermediates. In fact, in the most studied solid state reaction $\text{CO} + \text{H}$, the H bombardment of CO ices leads only to the observation of H_2CO and CH_3OH as the main reaction products. Being more reactive the reaction intermediates HCO and CH_3O are not observed (Watanabe et al. 2004). However $\text{CO} + \text{H}$ reaction investigated through neon matrix isolation has allowed the detection of HCO reaction intermediate (Pirim & Krim 2011). The results of the co-injection of CHOCHO diluted in neon gas ($\text{CHOCHO}/\text{Ne} = 1/100$) with H/H_2 mixture are shown in figure 6b. Additionally, the co-injection of CHOCHO diluted in neon gas ($\text{CHOCHO}/\text{Ne} = 1/100$) with H_2 molecules has been carried out (figure 6a) as a reference experiment in order to distinguish the reaction products derived specifically from $\text{CHOCHO} + \text{H}$ reaction isolated in neon matrix. The neon matrix isolation has been carried out at 3 K in order to freeze out all the species trapped in the rare gas crystal and then to avoid secondary reactions.

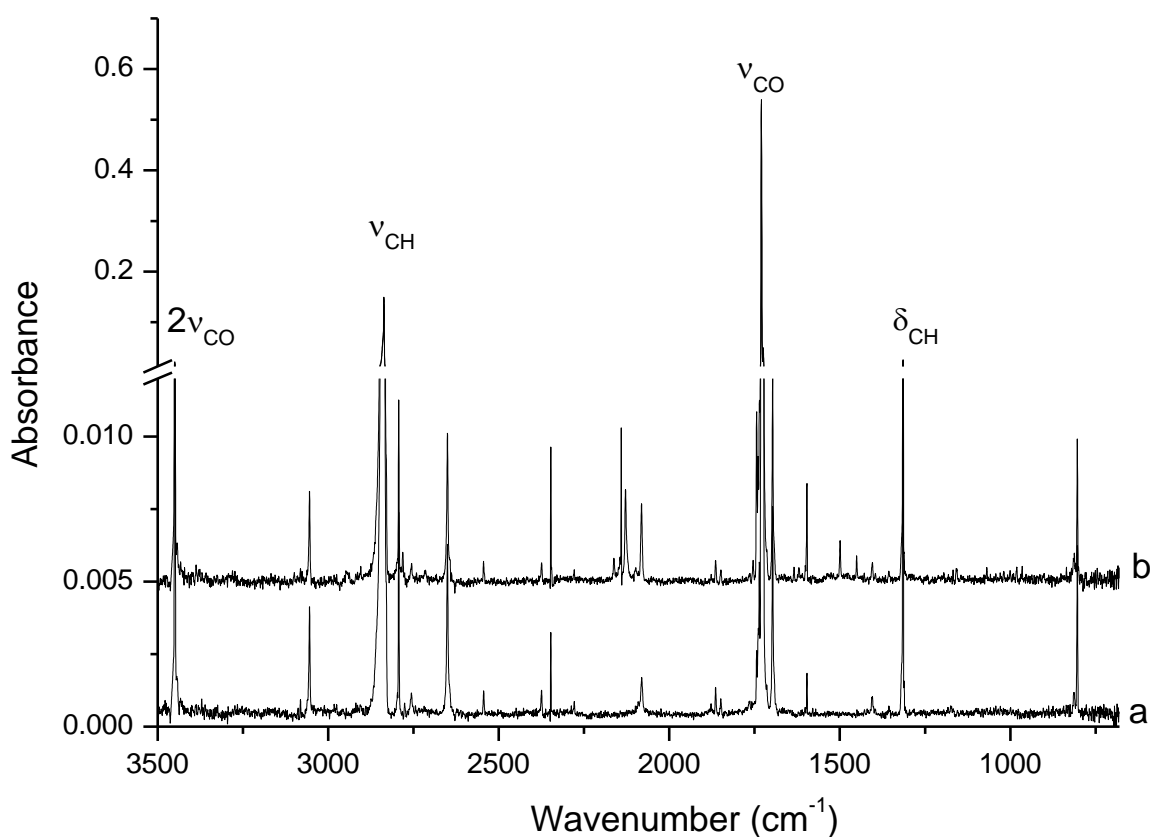


Figure 6: CHOCHO + H isolated in neon matrix at 3 K. a) Co-injection of CHOCHO/Ne (1/100) + H₂. b) Co-injection of CHOCHO/Ne (1/100) + H/H₂.

We notice that similar reaction products are observed in Exp 2 and Exp 3 through CHOCHO + H/H₂ and CHOCHO/Ne + H/H₂ co-injections, respectively. However, the neon matrix isolation method allows a clear separation between the IR signals due to glyoxal and those due to the reaction products. For example, in the CHOCHO + H/H₂ experiment the IR signal due to the CO vibrational mode of H₂CO is hidden by the wide absorption band of glyoxal ice as it is shown in figure 4. While, in the case of CHOCHO/Ne + H/H₂, the matrix isolation study allows a measurement of the IR signal of the CO functional group of H₂CO at 1744 cm⁻¹ as presented in figures 6 and 7 and which is in good agreement with previous studies carried out by Nelander who showed that the CO vibrational mode of formaldehyde isolated in rare gas matrix absorbs at 1744 cm⁻¹ (Nelander 1980). In fact, the analysis of figure 7 which is a zoom of figure 6 shows that all the IR signals located between 1700 and 1750 cm⁻¹ are due to CHOCHO trapped in the neon matrix. They have slightly the same IR intensities for CHOCHO/Ne + H/H₂ and CHOCHO/Ne + H₂ co-injection experiments. However the signal around 1744 cm⁻¹ is relatively more intense in the case of CHOCHO/Ne + H/H₂ co-injection

experiment and it may be assigned to H₂CO. The formation of H₂CO is also confirmed with the observation of the characteristic band of formaldehyde round 1500 cm⁻¹ (Nelander 1980). Additionally, another new signal is clearly measurable in the C=O functional group spectral region at 1755 cm⁻¹ (figure 7). This spectral region is characteristic of glycolaldehyde. Chin et al (2014) showed that glycolaldehyde isolated in neon matrix is mainly characterized by three strong IR absorption features at 1753, 1112 and 3544 cm⁻¹. Consequently one could think that the signal at 1755 cm⁻¹ would belong to glycolaldehyde formed during the CHOCHO/Ne + H/H₂ co-injection experiments and trapped in neon matrix. However, although we did not detect other new signals around 1112 and 3544 cm⁻¹ to confirm the formation of glycolaldehyde through CHOCHO + H reaction isolated in neon matrix, the signal at 1755 cm⁻¹ cannot be assigned to glycolaldehyde but to a reaction intermediate. In fact the heating of the neon matrix from 3 to 10 K leads to a decrease of the signal at 1755 cm⁻¹ while the signals at 1744 and 1500 cm⁻¹ attributed to H₂CO remain constant.

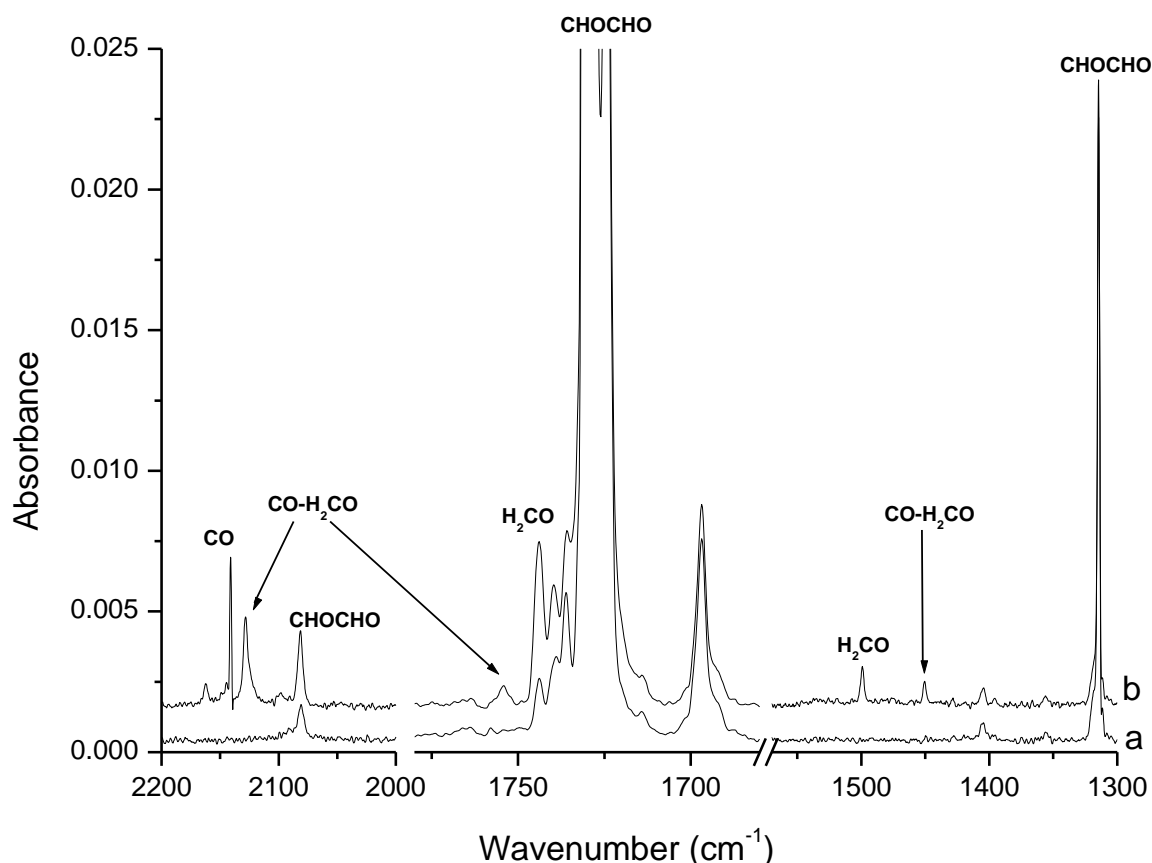


Figure 7: Zoom of figure 6, in three spectral regions, 2200-2000 cm⁻¹, 1780- 1680 cm⁻¹ and 1550-1300 cm⁻¹. a) CHOCHO + H₂ reaction. b) CHOCHO + H+ H₂ reaction.

As mentioned above, the neon matrix isolation study has been carried out to identify the nature of the CO-H₂CO reaction intermediate we have detected through the CHOCHO + H/H₂ co-injection experiments and which absorbs, as shown in figure 5, in the CO molecule region at 2115 cm⁻¹ and in the H₂CO region at 1450 cm⁻¹. In the case of CHOCHO/Ne + H/H₂ co-injection experiments, similar IR signals have been also observed at 2128 and 1451 cm⁻¹ in the CO and H₂CO molecules spectral regions. The three new signals observed in Exp 3 at 2128, 1755, 1451 decrease similarly when the neon matrix is heated and they would be related more to a same reaction intermediate than to a stable product. Compared to the band position of H₂CO at 1744 cm⁻¹, the new signal observed at 1755 cm⁻¹ shows a blue shift of +13 cm⁻¹. The signal at 2128 cm⁻¹ shows a red shift of +13 cm⁻¹ compared to CO molecule absorption band at 2141 cm⁻¹ and that at 1451 cm⁻¹ presents a red shift of +48 cm⁻¹ compared to the H₂CO bending position at 1499 cm⁻¹. The hypothesis is that these three absorption bands would correspond to the same CO-H₂CO reaction intermediate where CO is linked to H₂CO. Such an intermediate is formed during the hydrogenation of glyoxal through an H-addition-elimination reaction CHOCHO + H → CO-H₂CO + H. Additionally, another new signal at 2162 cm⁻¹ is observed only in the neon matrix isolation study (Figures 6 and 7). This signal detected in the spectral region of CO molecule has not been assigned to any species. It could be due to CO trapped in neon matrix and perturbed by its solid environment. Such a signal shows a very low IR intensity which remains constant during the heating of the neon matrix between 3 and 10 K and disappears completely at temperatures higher than 15 K. No other reaction intermediates such as H₂CO-CHO or HCO are observed under our experimental conditions. HCO has strong IR features at 2480, 1860 and 1080 cm⁻¹ (Milligan & Jacox 1969) and it has been already observed under the same experimental conditions in the case of CO + H isolated in neon matrix during the hydrogenation of CO (Pirim & Krim 2011). Consequently, no free or linked HCO is formed during the hydrogenation of glyoxal and the only probable reaction intermediate formed would be CO-H₂CO.

Although among the new signals observed in our IR spectra to monitor the CHOCHO + H reaction, no one might be assigned to glycolaldehyde or ethylene glycol, this cannot be a proof of their non-formation. They might form under our experimental conditions with very low amount leading to undetectable IR signals. Consequently, we cannot have a firm conclusion concerning the formation or non-formation of glycolaldehyde or ethylene glycol through CHOCHO + H reaction based only on the IR analysis. In order to have an obvious answer about the production of reaction products larger than CO and H₂CO, we have used the temperature programmed desorption (TPD) coupled to spectrometry to monitor the CHOCHO

+ H reaction products formed in the solid phase and released in the gas phase during the thermal desorption of the sample. The desorbing species are mainly identified by comparing the desorption temperatures and fragmentation patterns. Table 2 shows the characteristic m/z mass values of H₂CO, CH₃OH, CHOCH₂OH and HOCH₂CH₂OH and the relative intensities of mass fragments estimated from the literature for each species. We have measured under our experimental conditions the desorption temperature and fragmentation patterns of CHOCHO. Figure 8 shows the TPD results obtained during the heating of the sample formed by CHOCHO + H co-injection method to characterize H₂CO, CH₃OH, CHOCHO, CHOCH₂OH and HOCH₂CH₂OH through:

- The parent species at m/z = 30, 32, 58, 60, 62, respectively.
- The predominant fragments at m/z = 29, 31, 29, 31, 31, respectively.
- Other characteristic fragments at m/z = 28, 29, 30, 29, 33, respectively.

H₂CO desorbs at 95 K with (Chuang et al. 2016) a predominant fragment at m/z = 29 showing the greatest relative abundance. CH₃OH, CHOCH₂OH and HOCH₂CH₂OH desorb at 145, 195 and 214 K, respectively (Maity et al. 2015; Butscher et al. 2015). The predominant fragment of all these species is at m/z = 31.

Table 2: Characteristic m/z values of H₂CO, CH₃OH, CHOCHO, CHOCH₂OH and HOCH₂CH₂OH. Relative intensities of mass fragments are given in parenthesis

Species	H ₂ CO ^a	CH ₃ OH ^a	CHOCHO ^c	CHOCH ₂ OH ^b	HOCH ₂ CH ₂ OH ^b
Parent species m/z =	30 (70%)	32 (75%)	58 (31%)	60 (1%)	62 (3%)
Predominant fragment m/z =	29 (100%)	31 (100%)	29 (100%)	31 (100%)	31 (100%)
Other Fragments m/z =	28 (29%)	29 (61%)	30 (55%)	29 (50%)	33 (47%)
		30 (14%)	28 (28%)	32 (38%)	29 (36%)
		28 (9%)	31 (3%)	28 (12%)	32 (12%)
			32 (1%)	30 (6%)	30 (8%)
				28 (6%)	

^a(Fedoseev et al. 2015)

^b(Butscher et al. 2015)

^c Present work

From figure 8 we note that all the characteristic mass signals of CHOCHO (m/z = 58, 32, 31, 30, 29) start desorbing at 145 K, reach a maximum at 177 K and disappear at 185 K. It also

shows that the desorption of H_2CO characterized by the mass signals of the parent molecule at $m/z = 30$ (70%) and the predominant fragment at $m/z = 29$ (100%) occurs at 93 K. However, there is no evidence for CHOCH_2OH and $\text{HOCH}_2\text{CH}_2\text{OH}$ desorption which should occur in the 180 - 230 K temperature range. We do not detect mass signals due to the parent species at $m/z = 60$ (1%) or to the most characteristic fragments at $m/z = 31$ (100%) and 29 (50%) of CHOCH_2OH which should desorb around 195 K. Formed in low concentrations, CHOCH_2OH would also desorb at lower temperatures and it would be dragged into the gas phase during CHOCHO ice desorption. However, we have noticed that CHOCHO ice desorption shows the same relative intensities of the fragments with and without hydrogenation. Similarly, in the case of the $\text{HOCH}_2\text{CH}_2\text{OH}$, the desorption should take place around 214 K but we do not observe mass signals due to the parent species at $m/z = 62$ (3%) or to the most characteristic fragments at $m/z = 31$ (100%) and 33 (50%). This confirms our IR data and proves that CHOCH_2OH and $\text{HOCH}_2\text{CH}_2\text{OH}$ are not formed under our experimental conditions or they are formed in very low amounts which are below the limit of detection. Regarding the formation and desorption of methanol which can be characterized by mass signals at $m/z = 32, 31, 29$ and 30, the mass spectrometry cannot give additional information, as CH_3OH desorbs at 145 K while CHOCHO starts desorbing at 145 K and both species have the same fragments.

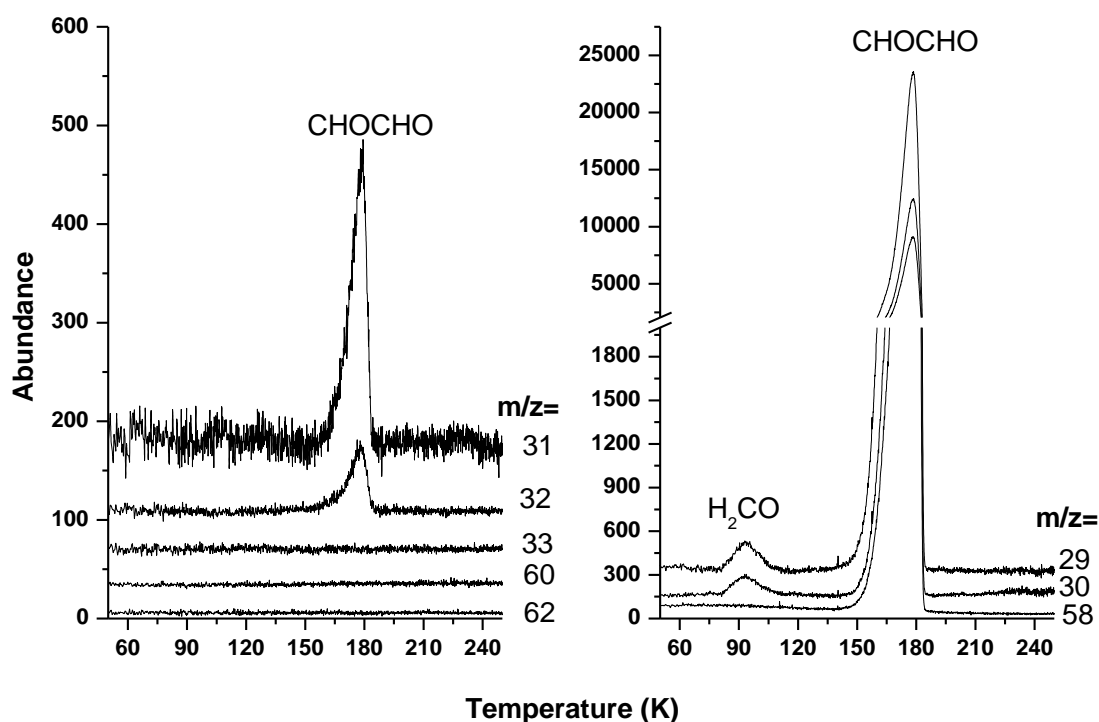


Figure 8: TPD spectra of glyoxal ice formed at 10 K through CHOCHO + H + H₂ co-injection experiment.

4 DISCUSSION

Using three experimental methods, we have investigated the CHOCHO + H solid state under non energetic conditions. We show that under our experimental conditions the hydrogenation of glyoxal cannot be the source of glycolaldehyde formation as often proposed by astrophysical models (Fedoseev et al. 2015, Wood et al. 2013) but is one of CHOCHO fragmentation leading to CO, H₂CO, CO-H₂CO reaction intermediate and probably CH₃OH. In order to answer how a non energetic processing (reactions occurring without supplying external energy such as UV photon or high energy particles) such as the H-addition reaction would dissociate CHOCHO instead of reducing one of the CO functional groups of glyoxal, one has to list how H atoms interact with CHOCHO molecule. In fact recent theoretical investigations carried out by Álvarez-Barcia et al. propose that the H-atom attack would occur in three different ways (Álvarez-Barcia et al. 2018) as illustrated in figure 9.

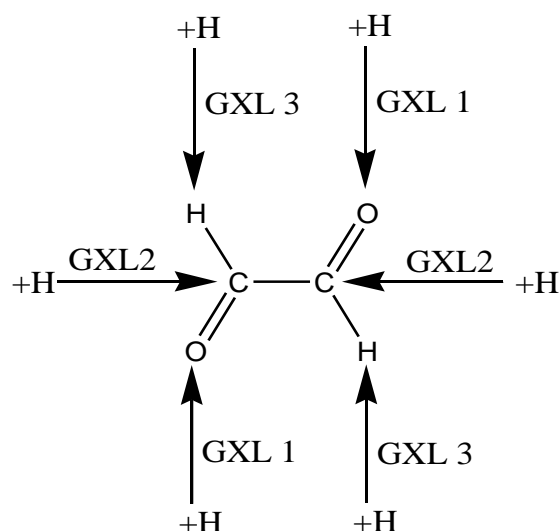


Figure 9: Schematic representation of glyoxal hydrogenation

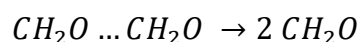
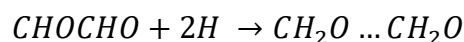
The GXL 1, GXL 2 and GXL 3 are the reaction pathways involving the three potential reactive centers of glyoxal, O, C and H, respectively, as follows:



Álvarez-Barcia et al suggest that glycolaldehyde would form through either GXL 1 or GXL 2 reaction pathways. The H-attack on CHOCHO would occur on one of the two oxygen atoms to form CHOHC[•]OH radical (GXL 1) or on one of the two carbon atoms to form CHOCH₂O[•] radical (GXL 2). These two radicals would react with additional hydrogen atoms to form CHOCH₂OH. However, the two reaction pathways GXL 1 and GXL 2 show two different energy barriers of 29.8 and 15.1 kJ/mol, respectively. The activation energy corresponding to the H-abstraction reaction of (GXL 3) to form H₂ and a radical species containing an aldehyde function and a carbonyl radical function has not been calculated. From these theoretical modelling of CHOCHO + H reaction, one would suggest that glycolaldehyde would form through GXL 2 reaction pathway. However, with the lack of the activation energy for the reaction pathway (GXL 3) and even though the H-attack on a carbon atom of glyoxal seems to be most favorable process for CHOCHO + H reaction, our experimental detection of CO and H₂CO during the glyoxal hydrogenation proves that the H-abstraction and molecular fragmentation compete with the H-addition processing. In this context, Zaverkin et al. (2018) suggest that both hydrogen addition and abstraction reactions play an important role as surface reactions in the chemical evolution of COMs in the molecular clouds of the ISM. They show by means of quantum chemical methods that in the case of CH₃CH₂CHO + H

reaction, the fastest mechanism by more than three order of magnitude is the H-abstraction from the CHO group and not the H-addition reaction which reduces CHO into CH₂OH. We propose then two reaction channels to explain the CHOCHO + H reaction. The first channel consists on a simultaneous formation of H₂CO during the glyoxal hydrogenation as follows:

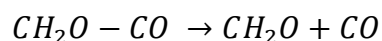
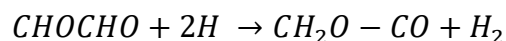
Channel 1:



As in CHOCHO, the two CHO functional groups are totally indiscernible, the H-atoms attack would occur simultaneously on the two carbon atoms to form an unstable intermediate CH₂O...CH₂O which will cause the C-C bond rupture and then a release of two formaldehydes. In comparison with the C-H bond (85 kcal/mol), the C-C bond (Koch et al, 2001; Feierabend et al, 2009) shows a lower bond dissociation energy (72 kcal/mol). Due to the high flux of the H-atoms such a process leading to a simultaneous attack of hydrogen atoms on the two carbons of CHOCHO may occur under our experimental conditions.

However, it may also occur successively, CHOCHO \xrightarrow{H} H₂CO-CHO \xrightarrow{H} 2H₂CO, with a very reactive reaction intermediate H₂CO-CHO which has not been experimentally detected. The mechanism we propose is similar to that proposed for the most studied solid state reaction CO + H where the H bombardment of CO ice leads to H₂CO through successive hydrogenation CO \xrightarrow{H} HCO \xrightarrow{H} H₂CO. Being very reactive, HCO is not observed during H-bombardment of CO ice (Watanabe et al 2004) and the global reaction is CO + 2H \rightarrow H₂CO. However, Channel 1 would give an explanation on the formation of H₂CO but not on that of CO. The second channel suggests that both the H-addition and H-abstraction reactions on the carbon atoms are energetically favourable, leading to the production of CO and H₂CO, the two reaction products we have detected experimentally.

Channel 2:



As hydrogen addition and abstraction reactions may compete, an H-abstraction would occur from one of the functional groups CHO while an H-addition process takes place on the other functional group CHO. This leads to the formation of formaldehyde (CH₂O), carbon monoxide (CO) and the reaction intermediate CH₂O-CO. Similarly, due to the high flux of the H-atoms under our experimental conditions such processes may occur simultaneously or successively. In fact based on Zaverkin et al. and Álvarez-Barcia et al. quantum calculations,

the first reaction step could be due to the H-abstraction $\text{CHOCHO} + \text{H} \rightarrow \text{CHO-CO} + \text{H}_2$. The H-addition would occur then on CHO-CO to form $\text{H}_2\text{CO-CO}$. Being very reactive, CHO-CO is not observed under our experimental conditions and the global reaction is $\text{CHOCHO} + 2\text{H} \rightarrow \text{H}_2\text{CO-CO} + \text{H}_2$. One would think that CHOCHO fragmentation would occur during the hydrogenation process leading to fragments such as HCO which interacting with H atoms would lead to H_2CO . However, we have not detected HCO during the $\text{CHOCHO} + \text{H}$ reaction and the only probable reaction intermediate we have observed would be $\text{CH}_2\text{O-CO}$ through a simultaneous H-addition-elimination reaction. This intermediate observed only during the Exp 2 and Exp 3, could be stabilized in glyoxal ice bulk or in neon matrix but not on the ice surface where it decomposes into H_2CO and CO . Finally, methanol formed during $\text{CHOCHO} + \text{H}/\text{H}_2$ co-injection is probably a secondary reaction product which forms through successive hydrogenation of the primary reaction product, the formaldehyde. This has been confirmed by additional experiments we have carried out by varying the H-atoms flux. We have noticed that the reducing of H-atoms flux in $\text{CHOCHO} + \text{H}/\text{H}_2$ co-injection experiments leads to a decrease of H_2CO yields and to a non-observation of CH_3OH . The formation pathways of methanol through $\text{H}_2\text{CO} + 2\text{H}$ are well known and have been highly investigated (Hiraoka et al. 1999, Watanabe & Kouchi 2002, Fuchs et al. 2009, Hama & Watanabe 2013).

The amounts of the reactant consumed (CHOCHO) and products formed (CO and H_2CO) have been evaluated from the IR spectra before and after H-bombardments of CHOCHO ice (figures 2a and 2b) and shown in table 3. The column densities N (molec cm^{-2}) of the reactant and products are directly deduced from integrated intensities of the corresponding characteristic absorption bands (Mencos et al. 2017). The column densities of glyoxal ice before and after H-bombardments have been calculated by probing the C=O stretching mode at 1709 cm^{-1} . The band strength value ($2.3 \times 10^{-17} \text{ cm molec}^{-1}$) found in the literature was measured in the gas phase but it is very close to band strength values of species with CHO functional group such as HCO (Bennett et al. 2005), H_2CO (Bouilloud et al. 2015) and CHOCH_2OH (Hudson et al. 2005) which have been measured in solid phase at 1.5×10^{-17} , 1.6×10^{-17} and $2.0 \times 10^{-17} \text{ cm molec}^{-1}$, respectively. This would give an order of magnitude of CHOCHO abundances. We found that just after sample deposition the amount of deposited glyoxal is $9.2 \times 10^{17} \text{ molec cm}^{-2}$. The H-bombardment of glyoxal during 45 min shows that only $2.1 \times 10^{16} \text{ molec cm}^{-2}$ of CHOCHO is consumed and consequently only 2.3 % of glyoxal react through $\text{CHOCHO} + \text{H}$ surface reaction. By including the contribution from the newly formed product H_2CO which has also an IR signal hidden by that of glyoxal in the ν_{CO} region, the yield of the reacting glyoxal is equal to 3.2 %. We have measured 6.3×10^{15} and $8.5 \times$

10^{15} molec cm^{-2} of CO and H_2CO , respectively, formed during the H-bombardments which leads to a concentration ratio $[\text{H}_2\text{CO}]/[\text{CO}] = 1.4$. We find that the total amount of the reaction products $[\text{H}_2\text{CO}] + [\text{CO}]$ is equal to 1.5×10^{16} molec cm^{-2} , while it should be 4.2×10^{16} molec. cm^{-2} if all the glyoxal consumed (2.1×10^{16} molec cm^{-2}) has been totally converted into H_2CO and CO. This shows that under the experimental conditions of Exp 1, only less than 35 % of the consumed glyoxal is transformed into H_2CO and CO. The other 65 % of the consumed glyoxal during the H-bombardments would either have desorbed during the H-bombardment or converted into reaction intermediates which have not been taken into account in these column density calculations.

Table 3: Column densities of reactants consumed (CHOCHO) and products formed (CO and H_2CO) during the glyoxal H-bombardment

	reactant consumed	Products formed	
Species	CHOCHO	CO	H_2CO
Mode	C=O stretch.	C=O bend.	CH_2 scis.
Position (cm^{-1})	1709	2144	1500
A (cm molec^{-1})	2.3×10^{-17} ^a	1.1×10^{-17} ^b	5.1×10^{-18} ^b
N (molec cm^{-2})	2.1×10^{16}	6.3×10^{15}	8.5×10^{15}

^a (Volkamer et al. 2005)

^b (Bouilloud et al. 2015)

We have compared the column densities calculated for CHOCHO + H surface reaction from Exp 1 to those obtained for the co-injection experiments Exp 2 and Exp 3. However, as for the co-injection experiments, the amounts of glyoxal consumed cannot be estimated, we have just focused on the column densities of the reaction products, as shown in Table 4.

Table 4: Column densities of reaction products formed during CHOCHO + H/ H_2 and CHOCHO/Ne + H/ H_2 co-injections.

	Exp 2			Exp 3	
Species	CO	H_2CO	CH_3OH	CO	H_2CO
Mode	C=O stretch.	CH_2 scis.	C-O stretch.	C=O stretch.	CH_2 scis.
Position (cm^{-1})	2143	1499	1030	2141	1499
A (cm molec^{-1})	1.1×10^{-17} ^a	5.1×10^{-18} ^a	1.1×10^{-17} ^a	1.1×10^{-17} ^a	5.1×10^{-18} ^a
N (molec cm^{-2})	5.8×10^{15}	9.6×10^{15}	3.1×10^{15}	8.1×10^{14}	1.3×10^{15}

^a Bouilloud et al. (2015)

The analysis of table 4 shows that the reaction product concentration ratios $[\text{H}_2\text{CO}]/[\text{CO}]$ are equal to 1.7 both for $\text{CHOCHO} + \text{H}/\text{H}_2$ and $\text{CHOCHO}/\text{Ne} + \text{H}/\text{H}_2$ co-injection experiments. This shows that experimental method would influence the $\text{CHOCHO} + \text{H}$ reaction pathways and change the branching ratios. Based on the two channels we propose, from one glyoxal molecule, we form either two H_2CO or one CO and one H_2CO . However in the case where both Channels 1 and 2 are equally probable, three H_2CO molecules would be formed versus one carbon monoxide which leads to $[\text{H}_2\text{CO}]/[\text{CO}] = 3$. While if Channel 2 is the only reaction pathway through $\text{CHOCHO} + \text{H}$ processing, one H_2CO molecule would be formed versus one carbon monoxide and then $[\text{H}_2\text{CO}]/[\text{CO}] = 1$. In both channels, CO and H_2CO are formed as primary reaction products, however under our experimental conditions, H_2CO could also be formed as a secondary product through successive hydrogenation of CO which will influence the final amount of H_2CO and CO and also $[\text{H}_2\text{CO}]/[\text{CO}]$ value. We have calculated the $[\text{H}_2\text{CO}]/[\text{CO}]$ for each experiment in order to find the final distribution of CO and H_2CO through $\text{CHOCHO} + \text{H}$ reaction. Compared to the Exp 1, the value of $[\text{H}_2\text{CO}]/[\text{CO}]$ ratio is higher in the Exp 2 (1.4 vs 1.7). Additionally, from Exp 2 we notice that $3.1 \times 10^{15} \text{ molec cm}^{-2}$ of H_2CO is converted into methanol under our experimental conditions. Taking this into consideration, we thus conclude that in the co-injection experiment the real reaction product concentration ratio $[\text{H}_2\text{CO}]/[\text{CO}]$ is equal to 2.2. We form more than two H_2CO versus one CO .

The hydrogenation of glyoxal under ISM conditions leads mainly to molecular fragmentation through H-abstraction processing, more efficient than the H-addition reaction to form glycolaldehyde or ethylene glycol starting from CHOCHO as reaction precursor. These chemical transformations of CHOCHO interacting with H atoms under non-energetic conditions without providing UV photons or high energy particles are sum up in figure 10.

Consequently, the hydrogenation of glyoxal to form glycolaldehyde or ethylene glycol is not efficient under our experimental conditions where the two species might be formed in low concentrations below the limit of our detection. We think that all these three species are more formed through radical recombinations during the interstellar formation or decomposition of methanol or formaldehyde which involve HCO, CH₃O and CH₂OH radical reactive species. The thermal reactions between these radical species would lead to the formation of many COMs (Bennett & Kaiser 2007, Butscher et al. 2015) such as CHOCHO, CHOCH₂OH and HOCH₂CH₂OH, through CHO + CHO, CHO + CH₂OH and CH₂OH + CH₂OH reactions, respectively.

However, the VUV photolysis of H₂CO carried out by Butscher et al. (2015) has shown that in contrast with CHO + CH₂OH and CH₂OH + CH₂OH radical recombination reactions which lead efficiently to glycolaldehyde and ethylene glycol, respectively, the formation of glyoxal through HCO + HCO dimerization is unfavoured. They explain the non-observation of CHOCHO by the fact that glyoxal, formed through CHO + CHO reaction, would promptly be hydrogenated and transformed into glycolaldehyde and ethylene glycol, as it is already proposed by many astrophysical models. This is in contradiction with our experimental results because the hydrogenation of glyoxal does not lead to detectable amounts of glycolaldehyde and ethylene glycol but to H₂CO and CO as primary and main reaction products. Recently, by combining matrix isolation of CHO radical and quantum chemical calculations, the same group (Butscher et al. 2017) shows that once it is formed by CHO + CHO thermally induced processing ($T > 45$ K), glyoxal would undergo an intra-molecular H-transfer leading to H₂CO + CO. They propose that H₂CO + CO may form through two steps CHO + CHO → CHOCHO → H₂CO + CO. However, while the first step consisting on CHO-CHO radical recombination to form glyoxal is exothermic by 70 kcal/mol, the second step shows a huge energy barrier of 55 kcal/mol. The authors suggest that CHOCHO would be formed in a high vibrational state with enough internal energy to overcome the energy barrier to form H₂CO + CO. Under our experimental conditions, there is no evidence for the CHO radical formation even through CHOCHO + H reaction isolated in neon matrix. The H₂CO and CO are formed in the 3-10 K temperature range more from an H-addition-elimination process on CHOCHO than CHO + CHO reaction.

5 CONCLUSION

More than 70 COMs have been detected in the ISM. However the formation reactions of many COMs are unknown. Various astrophysical models propose mechanisms for the formation of these complex molecules based on the abundances of species already detected. This is the case of glycolaldehyde and ethylene glycol which have been proposed to form by successive hydrogenation of glyoxal. In the context of explaining the formation of COMs in the ISM, we present here a study of glyoxal hydrogenation reactions carried out at 3 and 10 K. Our experimental results show that interacting with H-atoms under non-energetic conditions, glyoxal leads to the formation of formaldehyde, carbon monoxide and H₂CO-CO reaction intermediate. In addition, we have a tentative detection of methanol which could be a secondary reaction product resulting from the hydrogenation of formaldehyde. This allows us to propose reaction pathways for CHOCHO transformation under H-bombardments. Two reaction pathways have been proposed: channel 1 which leads to the formation of two formaldehydes and channel 2 which leads to the formation of H₂CO and CO. Consequently, the hydrogenation of glyoxal under ISM conditions would lead to molecular fragmentations through H-addition-abstraction processing, more efficient than the H-addition reaction to form glycolaldehyde or ethylene glycol.

REFERENCES

- Álvarez-Barcia S., Russ P., Kästner J., Lamberts T., 2018, *MNRAS*, 479, 2007
- Bacmann A., Faure A., 2016, *A&A*, 587, A130
- Beltrán M. T., Codella C., Viti S., Neri R., Cesaroni R., 2009, *ApJ*, 690, L93
- Bennett C. J., Jamieson C. S., Osamura Y., Kaiser R. I., 2005, *ApJ*, 624, 1097
- Bennett C. J., Kaiser R. I., 2007, *ApJ*, 661, 899
- Brouillet N., Despois D., Lu X.-H., Baudry A., Cernicharo J., Bockelée-Morvan D., Crovisier J., Biver N., 2015, *A&A*, 576, A129
- Bouilloud M., Fray N., Bénilan Y., Cottin H., Gazeau M.-C., Jolly A., 2015, *MNRAS*, 451, 2145
- Buckley P., Giguère P. A., 1967, *Can. J. Chem.*, 45, 397
- Butscher T., Duvernay F., Theule P., Danger G., Carissan Y., Hagebaum-Reignier D., Chiavassa, T., 2015, *MNRAS*, 453, 1587
- Butscher T., Duvernay F., Rimola A., Segado-Centellas M., Chiavassa, T., 2017, *PCCP*, 19, 2857
- Charnley S. B., Rodgers S. D., Ehrenfreund P., 2001, *A&A*, 378,1024
- Chin W., Chevalier M., Thon R., Polet R., Ceponkus J., Crépin C., 2014, *J. Chem. Phys.*, 140, 224319
- Chuang K.-J., Fedoseev G., Ioppolo S. van Dishoeck E. F., Linnartz H., 2016, *MNRAS*, 455, 1702
- Cole A. R. H., Durig J. R., 1975, *J. Raman Spectrosc*, 4, 31
- Cole A. R. H., Osborne G. A., 1971, *Spectrochimica Acta A*, 27, 2461
- Crovisier J., Bockelée-Morvan D., Biver N., Colom P., Despois D., Lis D. C., 2004, *A&A*, 418, L35
- Coutens A., Persson M., M. V., Jørgensen, J. K.; Wampfler, S. F.; Lykke, J. M., 2015, *A&A*, 576, A5
- Durig J. R., Hannum S. E., 1971, *J. Crys. Mol. Struct*, 1, 131
- Ewin G. E., Pimentel G. C., 1961, *J. Chem. Phys*, 35, 925
- Fedoseev G., Cuppen H. M., Ioppolo S., Lamberts T., Linnartz H., 2015, *MNRAS*, 448, 1288
- Frau P., Girart J. M., Beltrán M. T., 2012, *A&A*, 537, L9
- Fuchs G. W., Cuppen H. M., Ioppolo S., Romanzin C., Bisshop S. E., Anderson S., Linnartz H., van Dishoeck E. F., 2009, *A&A*, 505, 629
- Feierabend K. J., Flad J. E., Brown S. S., Burkhloeder J. B., 2009, *J. Phys. Chem. A*, 113, 7784
- Gerakines P. A., Schutte W. A., Greenberg J. M., van Dishoeck E. F., 1995, *A&A*, 296, 810
- Ha T.-K., 1972, *J. Mol. Struct*, 12, 171
- Hama T., Watanabe N., 2013, *Chem. Rev*, 113, 8783
- Herbst E., van Dishoeck E. F., 2009, *Annu. Rev. Astron. Astrophy.*, 47, 427
- Hiraoka K., Miyagoshi T., Takayama T., Yamamoto K., Kihara Y., 1999, *ApJ*, 498, 710
- Hollis J. M., Lovas F. J., Jewell P. R., 2000, *ApJ*, 540, L107
- Hollis J. M., Lovas F. J., Jewell P. R., Coudert L. H., 2002, *ApJ*, 571, L59
- Hudson R. L., Moore M. H., Cook A. M., 2005, *Adv Space Res*, 36, 184

Jørgensen J. K., Favre C., Bisschop S. E., Bourke T. L., Schmalzl M., van Dishoeck E. F., 2010, *ApJ*, 757, L4

Koch D. M., Khieu N. H., Peslherbe G. H., 2001, *J. Phys. Chem. A*, 105, 3598

Li Q.-S., Zhang F., Fang W.-H., Yu J.-G., J, 2006, *J. Phys. Chem.*, 124, 054324

Liszt H. S., Pety J., Gerin M., Lucas R., 2014, *A&A*, 564, A64

Maity S., Kaiser R. I., Jones B. M., 2015, *PCCP*, 17, 3081

Maté B., Gálvez O., Herrero V., Escribano R., 2009, *ApJ*, 690, 486

Mencos A., Nourry S., Krim L., 2017, *MNRAS*, 467, 2150

Milligan D. E., Jacox M. E., 1969, *J. Chem. Phys*, 51, 277

Muñoz Caro G. M., Jiménez-Escobar A., Martín-Gago J. Á., Rogero C., Atienza C., Puertas S., Sobrado J. M., Torres-Redondo J., 2010, *A&A*, 522, A108

Nelander B., 1980, *J. Chem. Phys*, 73, 1026

Palumbo M. E., Castorina A. C., Strazzulla G., 1999, *A&A*, 342

Pirim C., Krim L., 2011, *PCCP*, 13, 19454

Rivilla M. V., Beltrán M. T., Vasyunin A., Caselli P., Viti S., Fontani S., Cesaroni R., 2019, *MNRAS*, 483, 806

Schutte W. A., Allamandola L. J., Sandford S. A., 1993, *Science*, 259, 1143

Snyder L. E., Buhl D., Zuckerman B., Palmer P., 1969, *Phys. Rev. Lett*, 22, 679

Snyder L. E., Hollis J. M., Ulich B. L., 1976, *ApJ*, 208, L91

Stull D. R., 1947, *Ind. Eng. Chem. Res*, 39, 517

Taquet V., López-Sepulcre A., Ceccarelli C., Neri R., Kahane C., Charnley S. B., 2015 *A&A*, 804, 81

Volkamer R., Spietz P., Burrows J., Platt U., 2005, *J. Photochem. Photobiol. A*, 172, 35

Wang Y., Arif A. M., Gladysz J. A., 1994, *Organometallics*, 13, 2164

Watanabe N., Kouchi A., 2002, *ApJ*, 571, L173

Watanabe N., Nagaoka A., Shiraki T., Kouchi A., 2004, *ApJ*, 616, 638

Wood P. M., Slater B., Raza Z., Viti S., Brown W. A., Burke D. J., 2013, *ApJ*, 777, 90

Zaverkin V., Lamberts T., Markmeyer M. N., Kästner J., 2018, *A&A*, 617, A25